

Nonlinear ferromagnetic resonance induced by spin torque in nanoscale magnetic tunnel junctions

X. Cheng, J. A. Katine, G. E. Rowlands, and I. N. Krivorotov

Citation: [Applied Physics Letters](#) **103**, 082402 (2013); doi: 10.1063/1.4819179

View online: <http://dx.doi.org/10.1063/1.4819179>

View Table of Contents: <http://scitation.aip.org/content/aip/journal/apl/103/8?ver=pdfcov>

Published by the [AIP Publishing](#)



Re-register for Table of Content Alerts

Create a profile.



Sign up today!



Nonlinear ferromagnetic resonance induced by spin torque in nanoscale magnetic tunnel junctions

X. Cheng,^{1,2} J. A. Katine,² G. E. Rowlands,¹ and I. N. Krivorotov¹

¹Department of Physics and Astronomy, University of California, Irvine, California 92697, USA

²HGST, San Jose, California 95135, USA

(Received 28 May 2013; accepted 9 August 2013; published online 20 August 2013)

Spin transfer torque can excite ferromagnetic resonance of magnetization in a nanoscale magnetic tunnel junction. Here we describe a strongly nonlinear regime of spin-torque-driven ferromagnetic resonance in which large-amplitude magnetization oscillations are excited by microwave current applied to the junction. In this nonlinear regime, the junction generates a large direct voltage in response to the applied microwave signal and thereby can serve as a sensitive microwave signal detector. We demonstrate a low-temperature detector sensitivity of 2.5×10^4 V/W, which exceeds the sensitivity of metal-semiconductor Schottky diodes. © 2013 AIP Publishing LLC.

[<http://dx.doi.org/10.1063/1.4819179>]

The discovery of large tunneling magnetoresistance (TMR) in magnetic tunnel junctions (MTJs) with MgO tunnel barriers^{1–4} has led to the development of a variety of MTJ-based electronic devices such as non-volatile memory^{5,6} and hard drive read heads for high-density information storage.⁷ Recent experiments demonstrated that nanoscale MTJs can also rectify microwave signals⁸ and can thus function as microwave signal detectors.^{9,10} The rectified voltage V_{dc} generated by the MTJ originates from precession of the MTJ magnetization driven by alternating spin torque (ST) from the applied microwave signal.^{11,12} The maximum V_{dc} is observed when the frequency of the microwave signal is equal to the ferromagnetic resonance (FMR) frequency of the MTJ magnetization. Here we describe a different type of nonlinear magnetization dynamics excited by GHz-frequency ST in nanoscale MTJs, in which small-amplitude microwave signal with a frequency below the FMR frequency excites large-amplitude oscillations of magnetization. The rectified signals generated by the MTJ in this nonlinear regime exceed typical V_{dc} levels measured at the FMR frequency by nearly three orders of magnitude. This strong enhancement of the rectifying properties of nanoscale MTJs holds promise for the development of MTJ microwave signal detectors with sensitivity exceeding that of microwave Schottky diode detectors.

We study ST-driven magnetization dynamics in nanoscale MTJ samples schematically shown in Fig. 1(a). The samples have the following multilayer structure: (Si substrate)/(bottom lead)/(pinned layer)/(barrier)/(free layer)/(cap), where (pinned layer) \equiv PtMn(15)/Co₇₀Fe₃₀(2.5)/Ru(0.85)/Co₄₀Fe₄₀B₂₀(2.4), (barrier) \equiv MgO (1.1), and (free layer) \equiv Co₆₀Fe₂₀B₂₀ (1.56) with the layer thicknesses given in nanometers. The multilayers are grown by magnetron sputtering in a Singulus TIMARIS system and are annealed at 300 °C for 2 h in a 1 T in-plane magnetic field that sets the magnetization direction of the pinned layer. The multilayer is patterned into a 110×50 nm² elliptical nanopillar with the long axis parallel to the annealing field direction. For all measurements, a magnetic field is applied at 12° from the normal to the plane of the sample with its in-plane component along the direction of the magnetization of the Co₇₀Fe₃₀ layer,

as illustrated in Fig. 1(a). Fig. 1(b) shows the resistance of the sample, R , as a function of direct current, I_{dc} , applied between the top and the bottom leads of the nanopillar. ST from positive I_{dc} switches^{13–22} the magnetic moment of the MTJ free layer from the high-resistance (HR) state, a nearly antiparallel magnetic configuration at $I_{dc} = 0$ μ A, to the low-resistance (LR) state, a nearly parallel configuration at $I_{dc} \approx 100$ μ A (see Fig. 1(a)). The non-hysteretic character of the HR \leftrightarrow LR transition in Fig. 1(b) demonstrates that the free layer of the MTJ is superparamagnetic at 100 K.¹²

To study ST-driven GHz-range magnetization dynamics of the MTJ free layer, we apply an alternating current of RMS amplitude I_{ac} between the top and the bottom leads of the device and measure the direct voltage, V_{dc} , generated in response to the alternating current. ST from I_{ac} induces precession of the free layer magnetization, giving rise to resistance oscillations via the TMR effect. The time-dependent resistance takes on the form $R(t) \approx R_0(I_{ac}) + \delta R_{ac}(I_{ac}) \sin(\omega t + \varphi)$, where φ is the phase shift between the ac current and the resistance oscillations. As a result of mixing of the resistance and current oscillations, a rectified voltage $V_{dc} = \frac{1}{\sqrt{2}} I_{ac} \delta R_{ac} \cos(\varphi)$ is generated by the MTJ.⁹ In the presence of a direct current I_{dc} , the ac-ST induced direct voltage acquires an additional component proportional to I_{dc} because the time-average resistance of the MTJ, $R_0(I_{ac})$, depends on the alternating current by means of a shift of the time-average direction of the free layer magnetization induced by ST from I_{ac} .^{12,23} The induced direct voltage is thence given by $V_{dc} = \frac{1}{\sqrt{2}} I_{ac} \delta R_{ac} \cos \phi + I_{dc} \delta R_{dc}$, where $\delta R_{dc}(I_{ac}) = R_0(I_{ac}) - R_0(0)$ is the difference between the time-average MTJ resistance in the presence and in the absence of I_{ac} . To measure V_{dc} , we employ lock-in detection, in which the applied microwave signal is square-wave modulated, and the direct voltage induced by the microwave signal is measured by a lock-in amplifier.^{9,12}

Fig. 1(c) shows V_{dc} measured at zero direct current bias as a function of the frequency, f , of a 5 μ A RMS alternating current. This $V_{dc}(f)$ response curve shows a negative peak arising from FMR of the free layer excited by the alternating ST (ST-FMR).⁹ The observed resonance peak amplitude of tens of μ V is similar to that previously reported for MTJ

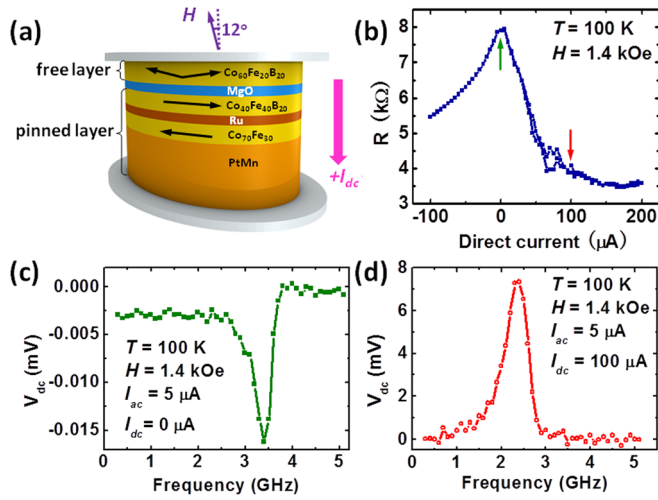


FIG. 1. Sample structure and ST-FMR spectra. (a) Schematic view of the MTJ nanopillar. (b) Resistance as a function of direct current I_{dc} applied to the MTJ. Arrows mark the direct current values at which ST-FMR measurements shown in (c) and (d) are made. (c) ST-FMR response curve $V_{dc}(f)$ measured at $I_{dc}=0 \mu\text{A}$. (d) ST-FMR response curve measured at $I_{dc}=100 \mu\text{A}$.

samples.^{9,24} Our measurements show that the maximum absolute value of $V_{dc}(f)$ can be significantly increased if a direct current bias is applied to the sample. Fig. 1(d) illustrates that application of $I_{dc}=100 \mu\text{A}$ reverses the sign of V_{dc} and increases the maximum V_{dc} by nearly three orders of magnitude as compared to the $I_{dc}=0 \mu\text{A}$ data in Fig. 1(c).

The origin of the large enhancement of V_{dc} can be understood by considering the magnetic energy landscape of the free layer nanomagnet. Fig. 2(a) schematically shows the magnetic energy E_M of the MTJ free layer as a function of the in-plane components of its magnetization $E_M(M_x, M_y)$.

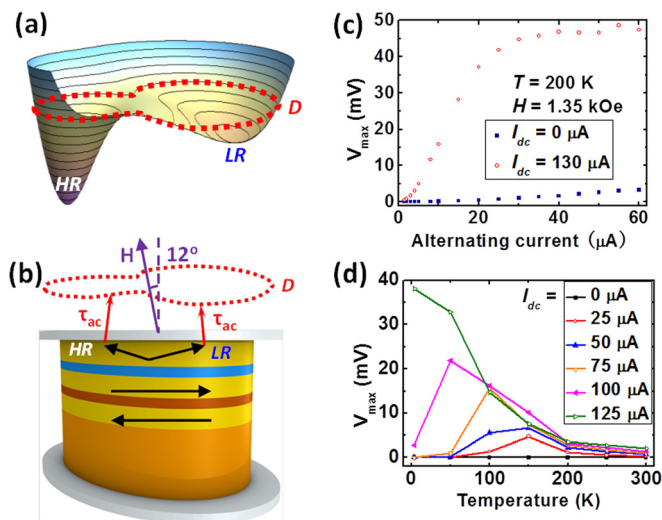


FIG. 2. Strongly nonlinear regime of ST-FMR. (a) Sketch of the magnetic energy of the free layer as a function of the in-plane component of its magnetization $E_M(M_x, M_y)$. Two energy minima correspond to the static LR and HR states while the large-amplitude trajectory of the magnetization corresponds to the dynamic state D. (b) Alternating ST, τ_{ac} , pushes magnetization towards the D state if the phase of the magnetization oscillations is π -shifted with respect to τ_{ac} . (c) $V_{\max} = \max\{V_{dc}(f)\}_{(f,H)}$ versus I_{ac} measured at $I_{dc}=0 \mu\text{A}$ and $I_{dc}=130 \mu\text{A}$. (d) Temperature dependence of the maximum voltage V_{\max} generated by the MTJ in response to a $5 \mu\text{A}$ RMS alternating current.

This energy landscape has two minima arising from the uniaxial magnetic shape anisotropy of the free layer. The global energy minimum corresponds to the HR state (favored by the in-plane component of the applied field) that is the ground state of the system at zero current (see Fig. 1(b)). Application of ST from a direct current ($I_{dc}=60 \mu\text{A}$ in Fig. 1(b)) brings the free layer into the higher-energy LR state corresponding to a shallow local energy minimum in Fig. 2(a). Fig. 2(a) also shows that at energies higher than that of the LR state, constant energy contours correspond to magnetization precession on large-amplitude out-of-plane trajectories encircling both the HR and LR states.²⁵ We argue that microwave currents with frequencies similar to the frequencies of these large-amplitude dynamic (D) states²⁶ bring the free layer from the static LR state into a D state. The frequency of the D-state trajectories can be significantly lower than the FMR frequency of small-amplitude oscillations in the HR state,¹⁶ which is in good agreement with our data in Figs. 1(c) and 1(d).

Coincidence of the drive frequency with the frequency of the D-state trajectory is not sufficient for excitation of the D state by alternating ST. Indeed, Gilbert damping torque acting on the free layer dissipates a significant amount of energy per oscillation period in the D state because the length of any D-state trajectory is large. Therefore, energy per cycle supplied by ST to the free layer magnetization must exceed a threshold value in order to sustain oscillations of magnetization in the D state.

Figure 2(b) illustrates that alternating ST supplies net positive energy to the D state provided the oscillations of the free layer magnetic moment are phase locked to the ac ST drive^{27,29} with approximately a π phase shift. For such phase-locked oscillations, ac ST pushes the magnetic moment of the free layer away from the HR state when the free layer is near the HR state ($I_{ac}\sin(\omega t) > 0$) and pushes magnetization towards the HR state (away from the LR state) when the free layer is near the LR state ($I_{ac}\sin(\omega t) < 0$). In both cases alternating current gives rise to a positive out-of-plane component of ST and, in turn, pushes the magnetic moment of the free layer towards the high-energy D trajectories above the plane of the sample. This net positive out-of-plane component of ST arising from the alternating current continuously pumps energy into the free layer nanomagnet. The positive energy flux from ST into the magnetic system in the D state counteracts the magnetic energy dissipation by Gilbert damping and thereby stabilizes the high-energy D state.

To supply energy per precession cycle exceeding a threshold value determined by Gilbert damping, ac ST must be sufficiently large. Therefore, we expect the D state to be stabilized only for I_{ac} exceeding a certain threshold value, which should result in a stepwise increase of V_{dc} from a small value below a threshold ac current to a large, nearly constant V_{dc} above the threshold. Fig. 2(c) shows the measured dependence of $V_{\max} = \max\{V_{dc}(f)\}_{(f,H)}$ on I_{ac} with and without the direct current bias. At zero dc current, the value of V_{\max} is small and $V_{\max}(I_{ac})$ is quadratic; this behavior shows that the D state is not excited at zero bias current. The observed quadratic dependence of V_{dc} on I_{ac} is expected because the amplitude of resistance oscillations δR_{ac} increases linearly with increasing ac ST drive in the regime

of small-amplitude magnetization oscillations:⁸ $V_{dc} \sim I_{ac} \delta R_{ac} \sim I_{ac}^2$. For $I_{dc} = 130 \mu\text{A}$, $V_{\max}(I_{ac})$ rapidly rises and saturates above $I_{ac,sat} \approx 30 \mu\text{A}$ at a large value of approximately 50 mV. This behavior differs from a step function, although any sharp step is smoothed in time-averaged $V_{dc}(I_{ac})$ by the action of thermal fluctuations, which randomly switch the system between the D state (large V_{dc}) and LR state (small V_{dc}) in the region of the LR \leftrightarrow D transition.

Because the D-state trajectory passes near both the HR and LR states, the time-average resistance of the D state, R_D , is approximately equal to the average of the LR and HR state resistances. Fig. 1(b) shows that $R_{LR} \approx 3.6 \text{ k}\Omega$ at $I_{dc} = 130 \mu\text{A}$, while the value of R_{HR} at $I_{dc} = 130 \mu\text{A}$ is approximately equal to resistance of the HR state at $I_{dc} = -130 \mu\text{A}$ ($R_{HR} \approx 5.0 \text{ k}\Omega$), which gives $R_D \approx 4.3 \text{ k}\Omega$. For $I_{dc} \gg I_{ac}$, $V_{dc} \approx I_{dc} \delta R_{dc}$ can be as high as $V_{dc} \approx I_{dc}(R_D - R_{LR}) \approx 90 \text{ mV}$. The values of V_{dc} in Fig. 2(c) are consistent with this upper bound on V_{dc} , demonstrating that magnetization oscillations with precession cone angle of tens of degrees are excited by ac ST at $I_{dc} = 130 \mu\text{A}$. We also note that ST from I_{dc} applied to the MTJ not only enhances V_{dc} but also supplies a fraction of the energy needed to stabilize the D state. Indeed, ST from $I_{dc} > 0$ pumps energy into the free layer as evidenced by I_{dc} -driven stabilization of the LR state, in which energy is higher than the ground (HR) state energy of the system. This also explains our observation that the saturation current $I_{ac,sat}$ decreases with increasing I_{dc} .

Observation of the D state excited by ac ST at a frequency lower than the HR-state FMR frequency is consistent with the energy landscape in Fig. 2(a). Low-energy D-state trajectories pass close to the separatrix trajectory separating the LR and D states. Since this trajectory passes through a saddle point in the energy landscape, it possesses zero frequency in the macrospin approximation. Therefore, frequencies of the D trajectories with energies slightly higher than that of the separatrix trajectory are low. Micromagnetic effects increase the frequency of the separatrix trajectory to a value greater than zero due to spatial inhomogeneity of the demagnetizing field, but the frequencies of the low-energy D trajectories remain lower than the FMR frequency in the HR state.

Our measurements reveal that excitation of the D state by low-level alternating current ($I_{ac} < I_{ac,sat}$) has a thermally activated character.^{28,29} Fig. 2(d) shows the temperature dependence of V_{\max} induced by a low-level alternating current $I_{ac} = 5 \mu\text{A}$ measured at several values of the direct current bias. The measured $V_{\max}(T)$ exhibits a peak, and the temperature of this peak decreases with increasing direct current. The data in Fig. 2(d) clearly show that a low-level alternating current does not excite the D-state when temperature is below a bias-dependent threshold temperature. Thus thermal fluctuations of magnetization are needed for initiation of the transition from the LR to the D state when $I_{ac} < I_{ac,sat}$. These data demonstrate that the maximum sensitivity of the MTJ detector can be tuned to a desired temperature by tuning the direct current bias. The data in Fig. 2(d) also suggest that phase locking between the ac ST drive and the magnetization oscillations in the D state is perturbed by random thermal torques, which results in a decrease of V_{dc} at higher temperatures. We

also note that $V_{\max}(T)$ at $I_{ac} = 125 \mu\text{A}$ does not exhibit a maximum because $I_{ac} = 5 \mu\text{A}$ ceases to be in the low-level regime since $I_{ac,sat} \approx 5 \mu\text{A}$ for $I_{dc} = 125 \mu\text{A}$ and $T = 4 \text{ K}$.

The observed phenomenon of large-amplitude oscillations of magnetization, excitation of which requires both a weak ac drive and temperature, is analogous to the well-known phenomenon of stochastic resonance.³⁰ In contrast to conventional stochastic resonance, we observe thermally activated excitation of a high-frequency dynamic state (non-adiabatic stochastic resonance)^{12,31,32} rather than quasi-periodic low-frequency transition between two static states.³⁰ The giant amplification of V_{dc} under a direct current bias was recently observed in all-metallic nanopillar spin valves,¹² in which the rectified signal arose from giant magnetoresistance (GMR). The maximum V_{dc} in these GMR structures was tens of μV , too low a value for practical microwave signal detection. The MTJ samples described in this paper generate maximum rectified voltages of tens of mV owing to the higher magneto-resistance of MTJs compared to that of GMR spin valves. We note that the higher magneto-resistance of MTJs enhances the rectified voltage not only via larger amplitude of resistance oscillations but also through additional alternating ST it generates in the large-amplitude precessional D state. Indeed, ST in MTJs is proportional to applied voltage,²⁴ and for a current-biased device, large-amplitude resistance oscillations result in alternating voltage at the frequency of magnetization precession. The alternating ST resulting from this voltage in the D state adds constructively to ST from the applied alternating current and thereby decreases the magnitude of the ac current needed to stabilize the D state.

Fig. 2(d) shows that the maximum induced dc voltage increases with increasing I_{dc} , and the largest detector sensitivity is found at the highest value of current bias employed in our measurements $I_{dc} = 125 \mu\text{A}$. For this direct current bias, the maximum rectified voltage of 40 mV is achieved at $T = 4 \text{ K}$ for $I_{ac} = 5 \mu\text{A}$, which gives detector sensitivity $\varepsilon = \frac{V_{dc}}{P_{in}} = 2.5 \times 10^4 \text{ V/W}$, where P_{in} is the incident microwave power. This value of the detector sensitivity exceeds that of high-sensitivity metal-semiconductor Schottky diode detectors³³ despite the poor impedance matching of our MTJ detector to the 50Ω transmission line through which microwave power is applied. Impedance matching of the detector can be improved by decreasing the resistance-area product of the MTJ and/or by adding a simple on-chip impedance matching transformer. The maximum expected sensitivity of an impedance matched MTJ sample is $\varepsilon = \frac{V_{dc}}{I_{ac}^2 R_D} \approx 3.6 \times 10^5 \text{ V/W}$. This value significantly exceeds the sensitivity of Schottky diode detectors as well as the maximum theoretical sensitivity of zero-bias MTJ detectors, 10^4 V/W .³⁴ We also note that increasing the volume of the free layer nanomagnet is expected to shift the temperature of maximum sensitivity at a given direct bias current (see Fig. 2(d)) to higher values¹² and thereby enable high-sensitivity room temperature operation of this type of microwave detectors.

In summary, we demonstrated excitation of a strongly nonlinear regime of spin torque ferromagnetic resonance in current-biased nanoscale MTJs in which large-amplitude out-of-plane magnetization precession is excited by alternating spin torque. In this nonlinear regime, direct voltage

generated by the MTJ in response to applied microwave signal is strongly enhanced compared to the linear regime of ferromagnetic resonance. Thus, current-biased MTJs hold promise for applications in microwave signal detection. We demonstrate a low-temperature detector sensitivity of 2.5×10^4 V/W.

This work was supported by NSF Grants (Nos. DMR-1210850, DMR-0748810, and ECCS-1002358) and by the FAME Center, one of six centers of STARnet, a Semiconductor Research Corporation program sponsored by MARCO and DARPA. We would like to thank Juergen Langer of Singulus Technologies for deposition of the magnetic multilayer used in this work. We also thank O. Prokopenko, A. Slavin, V. Tiberkevich, Y. Suzuki, and S. Yuasa for illuminating discussions on nonlinear ST-FMR.

- ¹W. H. Butler, X.-G. Zhang, T. C. Schulthess, and J. M. MacLaren, *Phys. Rev. B* **63**, 054416 (2001).
- ²J. Mathon and A. Umerski, *Phys. Rev. B* **63**, 220403(R) (2001).
- ³S. S. P. Parkin, C. Kaiser, A. Panchula, P. M. Rice, B. Hughes, M. Samant, and S.-H. Yang, *Nature Mater.* **3**, 862 (2004).
- ⁴S. Yuasa, T. Nagahama, A. Fukushima, Y. Suzuki, and K. Ando, *Nature Mater.* **3**, 868 (2004).
- ⁵W. J. Gallagher and S. S. P. Parkin, *IBM J. Res. Dev.* **50**, 5 (2006).
- ⁶J. M. Slaughter, *Annu. Rev. Mater. Res.* **39**, 277 (2009).
- ⁷P. P. Freitas, R. Ferreira, S. Cardoso, and F. Cardoso, *J. Phys: Condens. Matter* **19**, 165221 (2007).
- ⁸A. A. Tulapurkar, Y. Suzuki, A. Fukushima, H. Kubota, H. Maehara, K. Tsunekawa, D. D. Djayaprawira, N. Watanabe, and S. Yuasa, *Nature* **438**, 339 (2005).
- ⁹J. C. Sankey, P. M. Braganca, A. G. F. Garcia, I. N. Krivorotov, R. A. Buhrman, and D. C. Ralph, *Phys. Rev. Lett.* **96**, 227601 (2006).
- ¹⁰W. Chen, G. de Loubens, J.-M. L. Beaujour, J. Z. Sun, and A. D. Kent, *Appl. Phys. Lett.* **95**, 172513 (2009).
- ¹¹S. Ishibashi, T. Seki, T. Nozaki, H. Kubota, S. Yakata, A. Fukushima, S. Yuasa, H. Maehara, K. Tsunekawa, D. D. Djayaprawira, and Y. Suzuki, *Appl. Phys. Express* **3**, 073001 (2010).
- ¹²X. Cheng, C. T. Boone, J. Zhu, and I. N. Krivorotov, *Phys. Rev. Lett.* **105**, 047202 (2010).
- ¹³L. Berger, *Phys. Rev. B* **54**, 9353 (1996).
- ¹⁴J. C. Slonczewski, *J. Magn. Magn. Mater.* **159**, L1 (1996).
- ¹⁵J. A. Katine, F. J. Albert, R. A. Buhrman, E. B. Myers, and D. C. Ralph, *Phys. Rev. Lett.* **84**, 3149 (2000).
- ¹⁶S. I. Kiselev, J. C. Sankey, I. N. Krivorotov, N. C. Emley, R. J. Schoelkopf, R. A. Buhrman, and D. C. Ralph, *Nature* **425**, 380 (2003).
- ¹⁷W. H. Rippard, M. R. Pufall, S. Kaka, S. E. Russek, and T. J. Silva, *Phys. Rev. Lett.* **92**, 027201 (2004).
- ¹⁸S. Urazhdin, N. O. Birge, W. P. Pratt, and J. Bass, *Phys. Rev. Lett.* **91**, 146803 (2003).
- ¹⁹V. E. Demidov, S. Urazhdin, V. Tiberkevich, A. Slavin, and S. O. Demokritov, *Phys. Rev. B* **83**, 060406(R) (2011).
- ²⁰T. Devolder, J. Hayakawa, K. Ito, H. Takahashi, S. Ikeda, P. Crozat, N. Zerounian, Joo-Von Kim, C. Chappert, and H. Ohno, *Phys. Rev. Lett.* **100**, 057206 (2008).
- ²¹D. Houssameddine, U. Ebels, B. Delaët, B. Rodmacq, I. Firastrau, F. Ponthenier, M. Brunet, C. Thirion, J.-P. Michel, L. Prejbeanu-Buda, M.-C. Cyrille, O. Redon, and B. Dieny, *Nature Mater.* **6**, 447 (2007).
- ²²O. Boulle, V. Cros, J. Grollier, L. G. Pereira, C. Deranlot, F. Petroff, G. Faini, J. Barnas, and A. Fert, *Nat. Phys.* **3**, 492 (2007).
- ²³N. Mecking, Y. S. Gui, and C.-M. Hu, *Phys. Rev. B* **76**, 224430 (2007).
- ²⁴J. C. Sankey, Y.-T. Cui, J. Z. Sun, J. C. Slonczewski, R. A. Buhrman, and D. C. Ralph, *Nat. Phys.* **4**, 67 (2008).
- ²⁵R. Bonin, C. Serpico, G. Bertotti, I. D. Mayergoyz, and M. d'Aquino, *Eur. Phys. J. B* **59**, 435 (2007).
- ²⁶O. V. Prokopenko, I. N. Krivorotov, E. Bankowski, T. Meitzler, S. Jaroach, V. S. Tiberkevich, and A. N. Slavin, *J. Appl. Phys.* **111**, 123904 (2012).
- ²⁷Y. Zhou, J. Persson, S. Bonetti, and J. Åkerman, *Appl. Phys. Lett.* **92**, 092505 (2008).
- ²⁸D. M. Apalkov and P. B. Visscher, *Phys. Rev. B* **72**, 180405(R) (2005).
- ²⁹A. Slavin and V. Tiberkevich, *IEEE Trans. Magn.* **45**, 1875 (2009).
- ³⁰L. Gammaitoni, P. Hänggi, P. Jung, and F. Marchesoni, *Rev. Mod. Phys.* **70**, 223 (1998).
- ³¹G. Finocchio, I. N. Krivorotov, X. Cheng, L. Torres, and B. Azzzerboni, *Phys. Rev. B* **83**, 134402 (2011).
- ³²M. d'Aquino, C. Serpico, R. Bonin, G. Bertotti, and I. D. Mayergoyz, *Phys. Rev. B* **84**, 214415 (2011).
- ³³E. R. Brown, A. C. Young, J. Zimmerman, H. Kazemi, and A. C. Gossard, *IEEE Microwave Mag.* **8**, 54 (2007).
- ³⁴C. Wang, Y.-T. Cui, J. Z. Sun, J. A. Katine, R. A. Buhrman, and D. C. Ralph, *J. Appl. Phys.* **106**, 053905 (2009).